We are IntechOpen, the world's leading publisher of Open Access books Built by scientists, for scientists

5,300
Open access books available

130,000
International authors and editors

155M
Downloads

Our authors are among the

154
Countries delivered to

TOP 1%
most cited scientists

12.2%
Contributors from top 500 universities

CLARIVATE ANALYTICS BOOK CITATION INDEX INDEXED

WEB OF SCIENCE™

Selection of our books indexed in the Book Citation Index in Web of Science™ Core Collection (BKCI)

Interested in publishing with us?
Contact book.department@intechopen.com

Numbers displayed above are based on latest data collected.
For more information visit www.intechopen.com

Chapter

Gd_2O_3: A Luminescent Material

Raunak Kumar Tamrakar and Kanchan Upadhyay

Abstract

Luminescence behavior of the Gd_2O_3 phosphor is one of the important aspects in the technology of rare earth-based inorganic phosphor materials. The structural and optical behavior of a Gd_2O_3 nanophosphor will be discussed in detail. Structural characterization of the Gd_2O_3 was carried out via X-ray diffraction and electron microscopy methods. To detail the photoluminescence behavior, the excitation and emission spectra were recorded and discussed. Thermoluminescence (TL) study and kinetic analysis of the UV- and gamma-irradiated phosphor were also carried out to determine the use of the phosphor for the dosimetric application. Tunned glow peaks were deconvoluted by applying glow curve deconvolution function, and all the trapping parameters were determined.

Keywords: Gd_2O_3, combustion synthesis method, XRD, SEM, TEM, thermoluminescence, photoluminescence

1. Introduction

These days, rare earth oxide luminescent materials have pulled in incredible consideration because of their size, shape, and phase-dependent luminescent behavior, which make them reasonable for various applications. Among various groups of crystalline materials, oxide crystal is of incredible enthusiasm because of their exceptional optical properties, for example, long fluorescent lifetime, extensive Stokes shift, positive physical and chemical properties, and also great photochemical stability. A few of the rare earth components and their relating oxides are of exceedingly specialized significance and are utilized in basic parts. Rare earth oxides are this sort of cutting edge materials, which are generally utilized as elite luminescent gadgets, magnets, catalyst, and other useful materials, for example, electronic, attractive, atomic, optical, and synergist gadgets [1].

Lanthanide hydroxides and oxides have effectively been examined as a result of their extensive variety of utilizations including dielectric materials for multilayered capacitors, luminescent lights and shows, strong laser gadgets, optoelectronic information stockpiles, and waveguides. Lanthanide-doped oxide nanoparticles are of unique interests as potential materials for a vital new class of nanophosphors. At the point when connected for a fluorescent naming, they present a few focal points, for example, sharp emanation spectra, long-life times, and obstruction against photobleaching in examination with ordinary natural fluorophores and quantum spots [1, 2].

Gadolinium oxide (Gd_2O_3) is one of the good choices to researchers for luminescence behavior because it has high refractive index (2.3), high optical transparency, great thermal and chemical stability, high dielectric consistent, and low phonon energy among the group of oxide [3–6]. Due to these positive properties, it displays

various applications, for example, oxygen gas sensors, anode materials for sensors, optoelectronic gadgets, high definition TVs, medical imaging, high temperature superconducting materials, phenomenal UV light safeguard, photograph impetus, remedial impacts on malignant growth treatment-improving the impact of radiation on destructive cells while diminishing harm to typical cells, luminescent inks, paint and color sunscreen beautifiers, and luminescent materials [7].

Gadolinium oxide-based nanophosphors are observed to guarantee hopefuls in the field of superior luminescent gadgets, catalysis, and other practical gadgets dependent on their great electronic, optical, and physico-concoction reactions emerging from 4f electrons. Of course, every one of these properties could be to a great extent affected by their synthetic synthesis, precious stone structure, shape, and dimensionality. In this way, high surface region nanomaterial, which has a bigger part of deformity locales per unit zone, ought to be of enthusiasm as adsorbents in ecological remediation forms. Cost of amalgamation, effortlessness, and morphological attributes of arranged phosphor are vital parameters for their utilization in the business applications as it is basic that a self-spreading ignition course offers the best decision for the blend of Gd_2O_3 powder [2, 7].

Nanoparticles arranged by combustion synthesis have size of ~10 nm; such methodologies include the utilization of organic fuels such as urea, glycine, and so forth to start deterioration response of precursor metal salt at high temperature. The higher reactivity of littler size Gd_2O_3 particles is not simply because of the vast explicit surface region, yet in addition, because of the high concentration of low planned destinations and basic imperfections on their surface. Because of these benefits, these are sought after for different innovative applications including optoelectronic gadgets, top quality TVs, organic imaging and labeling, MRI, luminescent paints and inks for security codes, and so forth [8].

In the present work, combustion synthesis has been used for preparation of gadolinium oxide by utilizing glycerin and urea as a fuel. The union and portrayal of gadolinium oxide through various strategies have pulled in impressive consideration. The fuel and metal nitrate get deteriorated and give combustible gases, for example, NH_3, CO_2, and NO_2. At the point when the arrangement achieves a point of sudden ignition, it starts consuming and turns into a consuming strong. The ignition proceeds until the point that all the combustible substances have wore out, and it ends up being a free substance with voids and pores framed by the getting away gases amid the burning response. The entire procedure takes just a couple of minutes to yield powder of oxide. The auxiliary and optical portrayals of the incorporated powders were completed utilizing X-beam powder diffractometer. Checking electron microscopy (SEM) was utilized to show the development of crystallites, and TEM was utilized for molecular measure affirmation. Fourier Transform Infrared Spectroscopy (FTIR) range of Gd_2O_3 nanopowder was acquired by utilizing FTIR spectrophotometer (Model; MIR 8300TM) with KBr blend in the pellet shape. The Raman and X-ray photoelectron spectroscopic studies of the prepared phosphor were also carried out.

2. Materials and methods

2.1 Synthesis

Phosphor was synthesized by combustion synthesis method. Gadolinium nitrate was used as precursor solution and urea or glycine as fuel. Aqueous solution of gadolinium nitrate was prepared by dissolving suitable amount of precursor into

double distilled water followed by the addition of fuel. The mixture was kept in a magnetic stirrer at 60°C and stirred for 4 h, and a transparent gel was obtained. Gel was transferred into alumina crucible and kept in a preheated furnace at 600°C. The gel mixture undergoes dehydration followed by spontaneous combustion to form Gd_2O_3 powder [1, 2]. The resulting brownish powder was heated until a controlled explosion took place yielding a very fine, white powder. Since the reaction is so rapid, the crystal growth will be highly restrained (**Figures 1** and **2**).

2.2 Material characterization

The crystallinity of the phosphor was checked by X-ray diffraction estimation. The X-ray powder diffraction information was gathered by utilizing Bruker D8 Advanced X-ray diffractometer using Cu Kα radiation. The X-beams were created utilizing a fixed cylinder, and the wave length of X-beam was 0.154 nm. The X-rays were identified utilizing a quick checking indicator dependent on silicon strip technology (Bruker Lynx Eye finder). The surface morphology of the phosphors was detected by field emission electron microscopy (FESEM) JSM-7600F. Energy dispersive X-ray examination (EDX) was utilized for compositional investigation of the phosphor. Crystal size of arranged phosphor was determined by Transmission Electron Microscopy (TEM) utilizing Philips CM-200. Raman spectra were recorded by Jobin-Yvon, France, Ramnor HG-2S Spectrometer with Ar-Laser with 4 W control having goals of 0.5 cm^{-1} and wave number exactness of 1 cm^{-1} over 5000 cm^{-1}. XPS investigation was performed in a VG instrument with a CLAM2 analyzer and a twin Mg/Al anode. The weight pressure in the investigation chamber was roughly 9×10^{-10} mbar. The estimations were done with unmonochromated Al Kα photons (1486.6 eV). The intensity of the X-ray source was kept steady at 300 W.

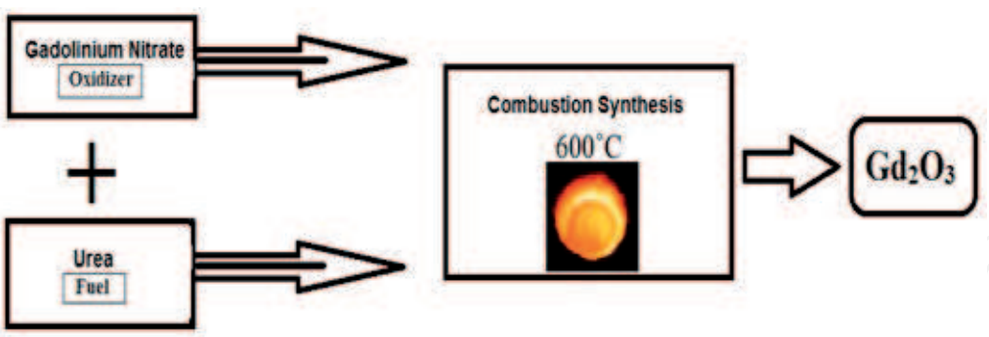

Figure 1.
Flow chart of synthesis of Gd_2O_3 with urea (reproduced from [1]).

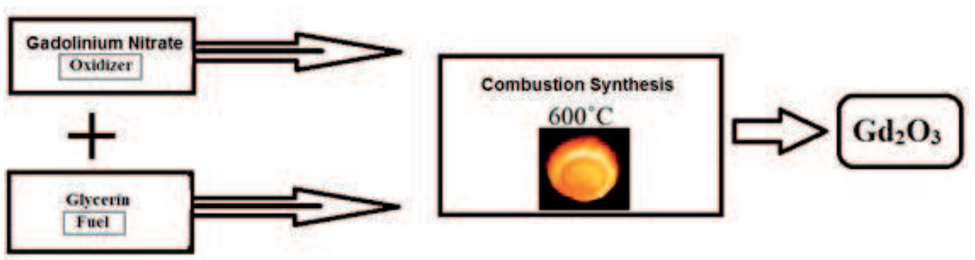

Figure 2.
Flow chart of synthesis of Gd_2O_3 with glycerin (reproduced from [2]).

3. Result and discussion

3.1 XRD result

The XRD pattern of the Gd_2O_3 sample is shown in **Figure 3**. The diffraction patterns are well matched with standard JCPDS card no. 43-1015, indicating that the sample of Gd_2O_3 phosphor is in the pure monoclinic phase. The particle size was calculated by the Scherer formula [7]

$$D = \frac{k\lambda}{\beta Cos\theta} \quad (1)$$

where D is the volume weighted crystallite size, k is the shape factor (0.9), λ is the wavelength of Cu Kα1 radiation, β_{hkl} is the instrumental corrected integral breadth of the reflection (in radians) located at 2θ, and θ is the angle of reflection (in degrees) utilized to relate the crystallite size to the line broadening. The average crystallite size of Gd_2O_3 nanoparticles was found to be in the range of 8–10 nm for both the fuels. No impurity peaks or other possible phases of Gd_2O_3 were observed. Further, the strong and sharp diffraction peaks confirm the high crystallinity of the products.

3.2 Surface morphology

The scanning electron microscopy (SEM) was utilized as a focused ray of high energy electrons to produce an assortment of signs at the crystalline surface.

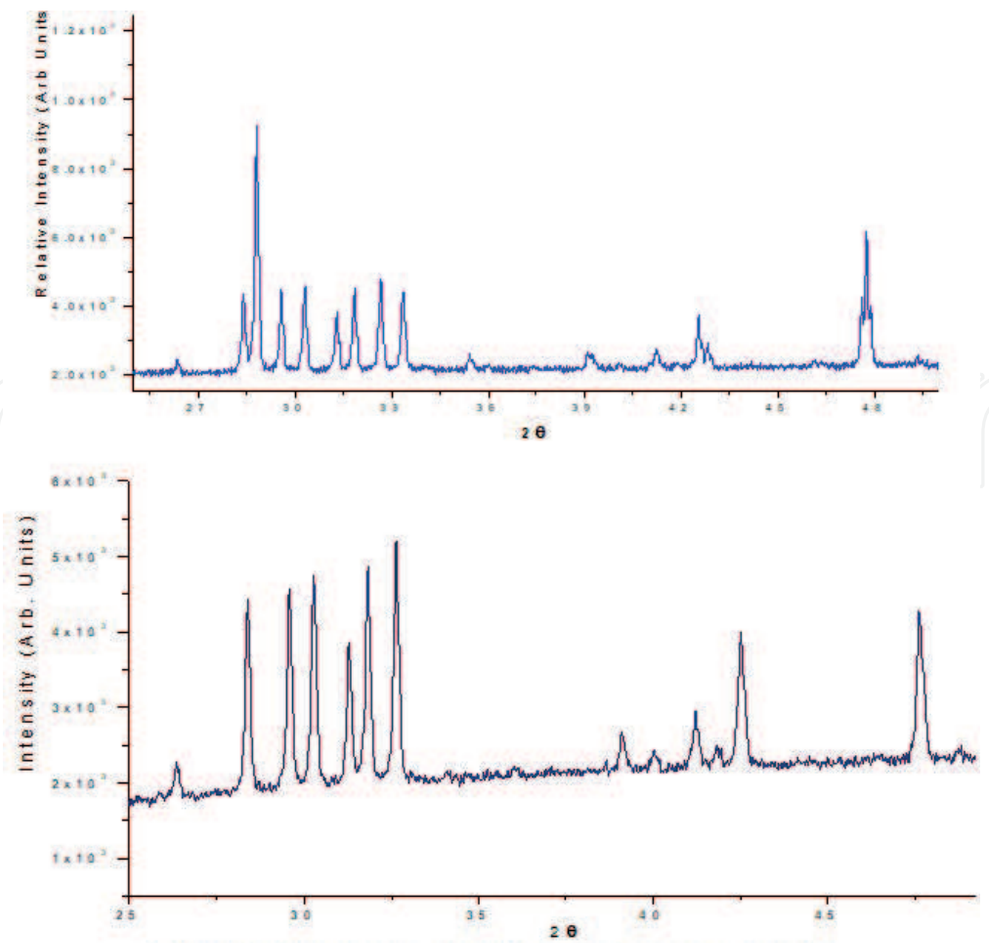

Figure 3.
XRD patterns of Gd_2O_3: (A) glycerin fuel and (B) urea fuel.

The signs that get from electron and sample interaction uncover data about the example including outer morphology, elemental composition, and crystalline structure and introduction of materials making up the example. The SEM is likewise fit for performing examinations of chose point areas on the example; this methodology is particularly valuable in subjectively or semi-quantitatively deciding synthetic structures. **Figure 4** demonstrates the SEM micrographs of the Gd_2O_3 arranged by combustion synthesis method utilizing urea and glycine as a fuel. The black and white SEM micrograph of the prepared powder indicates that all the particles are looking like agglomerated in homogeneously in different shapes/sizes of the order of nano range.

3.3 TEM result

Transmission electron microscopy (TEM) is an imaging system whereby a light emission is engaged onto an example making a broadened form show up on a fluorescent screen or layer of photographic film or to be distinguished by a CCD camera. The main commonsense transmission electron magnifying instrument was built by Albert Prebus and Lames Hillier at the college of Toronto in 1938 utilizing ideas grew before by Max Knoll and Ernst Ruska. The particle size of the system was determined by high resolution transmission electron microscopy (HRTEM). It is a phase differentiated imaging process because the image formed is due to the scattering of electron waves through a thin surface. In **Figure 5**, HRTEM micrograph demonstrates a Gd_2O_3 nanocrystal with a width of 8–10 nm seen all through the particle for both fuels [1, 2, 7].

3.4 Energy dispersive X-ray analysis (EDX)

Elemental investigation of the prepared samples is generally determined by EDX analysis. The spectrum shows the relation between the X-ray energy, which lies in between 10 and 20 eV, and the number of counts per channel by a plot between them in X and Y axes, respectively. An X-ray line is expanded by the reaction of the framework, delivering a Gaussian profile. Energy resolution is characterized as the full width of the crest at half maximum height (FWHM). In the spectrum of both the Gd_2O_3 samples, intense peak of Gd and O is present, which confirms the formation of Gd_2O_3 phosphor (**Figure 6**). For EDX analysis, the entire area of the black and white SEM micrographs was analyzed with EDX mapping and spectrum. The

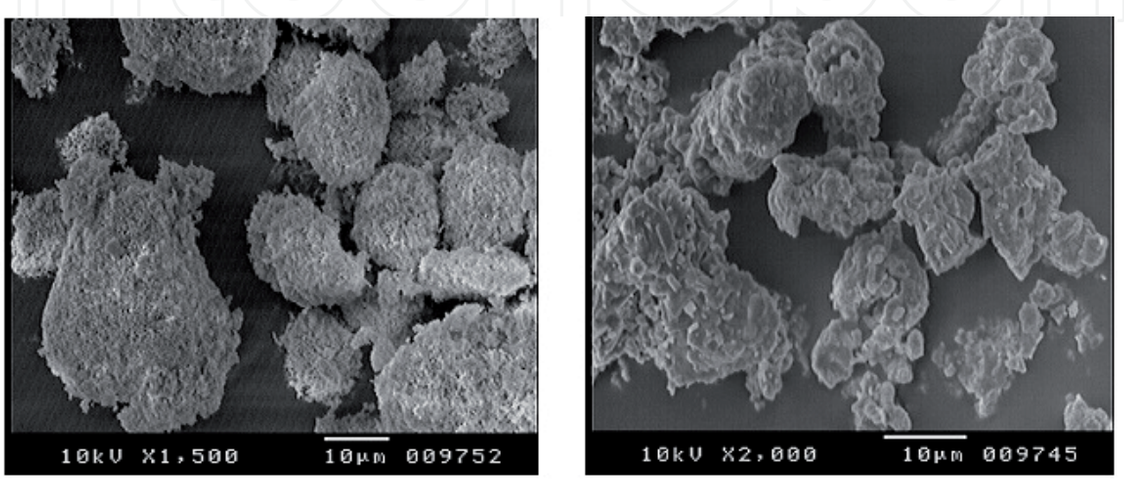

Figure 4.
Scanning electron microscope image of Gd_2O_3 phosphor: (A) glycerin fuel and (B) urea fuel.

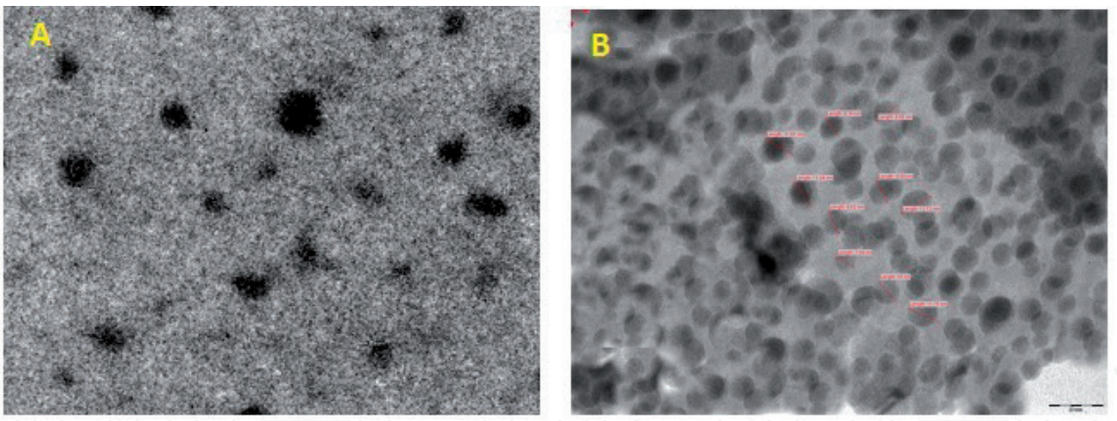

Figure 5.
Transmission electron microscope image of Gd_2O_3 phosphor: (A) glycerin fuel and (B) urea fuel.

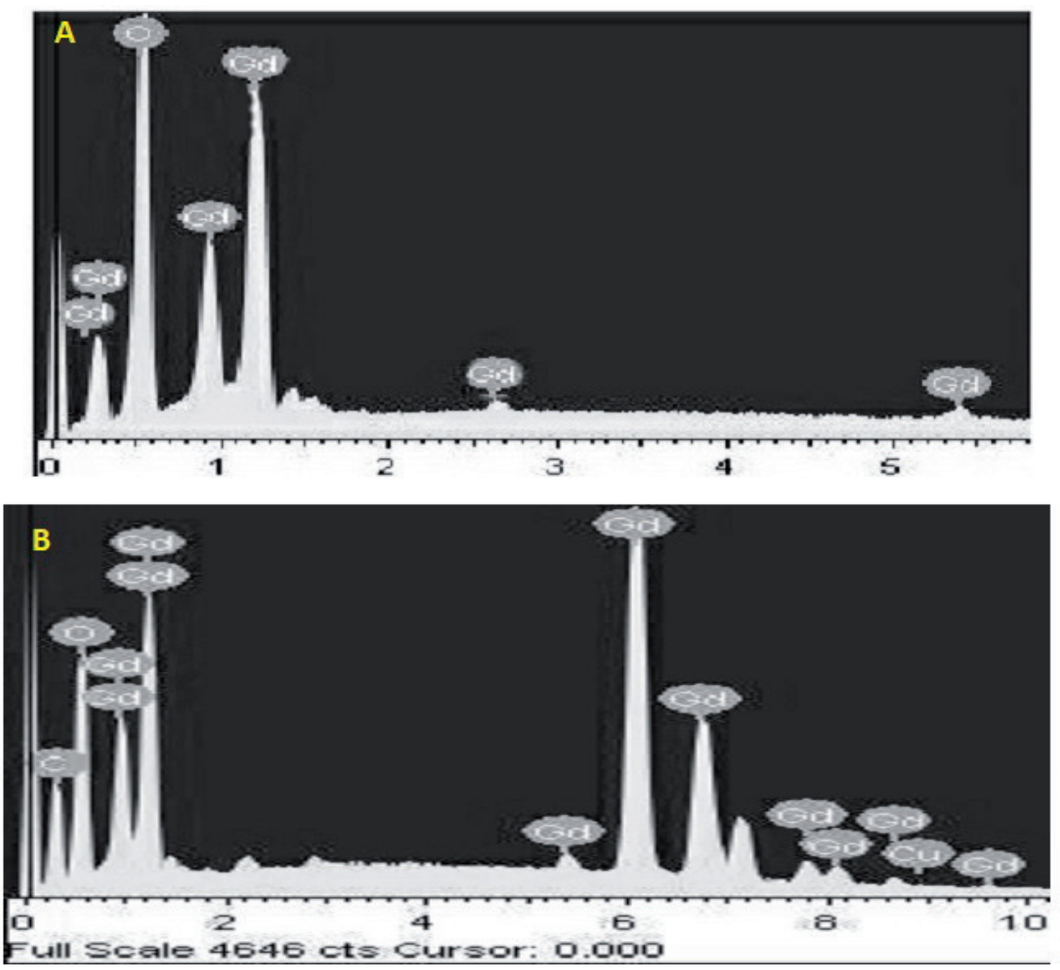

Figure 6.
EDX spectra of Gd_2O_3 phosphor: (A) glycerin fuel and (B) urea fuel.

EDX mapping measurements were carried Gd_2O_3 powders to analyze the composition of the clustered particles [1, 2].

3.5 X-ray photoelectron spectroscopy (XPS)

XPS is a surface compositional investigation system that can be utilized to examine the surface chemistry of a material in its as-formed state, or after some treatment, for instance: cracking, cutting, or scratching in air or UHV to uncover the bulk chemistry, ion beam etching to wipe off a few or the majority of the surface

defilement or to purposefully uncover further layers of the sample inside and out profiling XPS, presentation to warmth to think about the progressions because of warming, introduction to receptive gases or arrangements, introduction to particle bar embed, and introduction to bright light. The synthetic organization of Gd_2O_3 nanoparticles was contemplated with X-ray Photoelectron Spectroscopy (XPS), and the test information was broken down utilizing bend fitting. The Gd (3d) level comprised of a turn circle split with the Gd (3d)5/2 top is found at 1186.74 eV (**Figure 7**). The line shape and pinnacle positions are in great concurrence with prior distributed information on Gd_2O_3 powder squeezed into the sheet [1].

3.6 Raman spectroscopy

To understand the molecular structure, Raman effect has been used, and the obtained Raman data can be compared with the infrared spectra. Raman spectroscopy is very informative to illustrate the structure of the phosphor. It is a nondestructive device to investigate vibrational, rotational, and other low recurrence modes in the frameworks under study. **Figure 8** demonstrates the Raman spectra of Gd_2O_3 obtained by combustion synthesis method. The spectra were recorded at room temperature with an excitation wavelength of 633 nm He-Cd laser. An broad and intense Raman crest at 340 cm^{-1} along with less extreme peaks was seen at 375, 395, 424, and 451 cm^{-1}. The outcomes are in great concurrence with the recently distributed Raman spectroscopic examinations on Gd_2O_3 nanoparticles [1].

3.7 Photoluminescence spectra and CIE diagrams of Gd_2O_3 phosphors

The emission spectra of Gd_2O_3 phosphor prepared with both the fuels have emission peaks at UV and visible region. A slight variation in peaks was observed in emission peaks for both phosphors. The emission spectra of Gd_2O_3 phosphor prepared by combustion synthesis method have peak at UV region in between 317 and 399 nm along with weak blue band around 450–494 nm, green around 515–586 nm, and red emission centered at 616–625 nm (**Figure 9**).

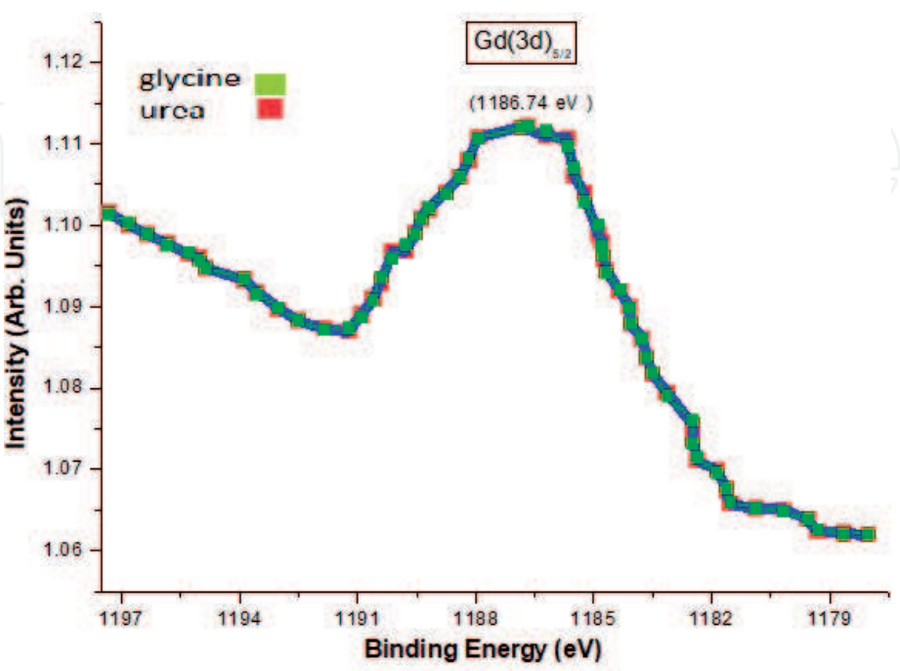

Figure 7.
The Gd (3d) XPS spectrum of Gd_2O_3 nanocrystals (reproduced from [1]).

$^6P_{7/2} \rightarrow {}^8S_{7/2}$ transition is responsible for the UV emission centered at 317 nm, whereas the visible emissions are due to transition from ^6G_J state of Gd^{3+} [8]. The presence of oxygen vacancy and interstitials also contributes in modified photoluminescence response for oxide-based system [8]. Transition from ^6G_J state of Gd^{3+} ion and $^6G_J/^6P_J$ transition is responsible for green and red emissions, respectively (**Figure 10**).

To determine the specific color produced by the prepared Gd_2O_3 phosphor, CIE coordinate diagram was prepared by using MATLAB 7.10.0 (R2010a) software. The CIE coordinates for combustion synthesized Gd_2O_3 phosphor were found $X = 0.207$ and $Y = 0.206$, which resemble with blue color. Effect of annealing on the produced color was determined by the CIE coordinates of Gd_2O_3 phosphor annealed at 900°C. It was observed that the X and Y coordinates for the annealed sample have same values as freshly prepared samples, and only the change in intensity was observed after annealing (**Figure 9**) [9].

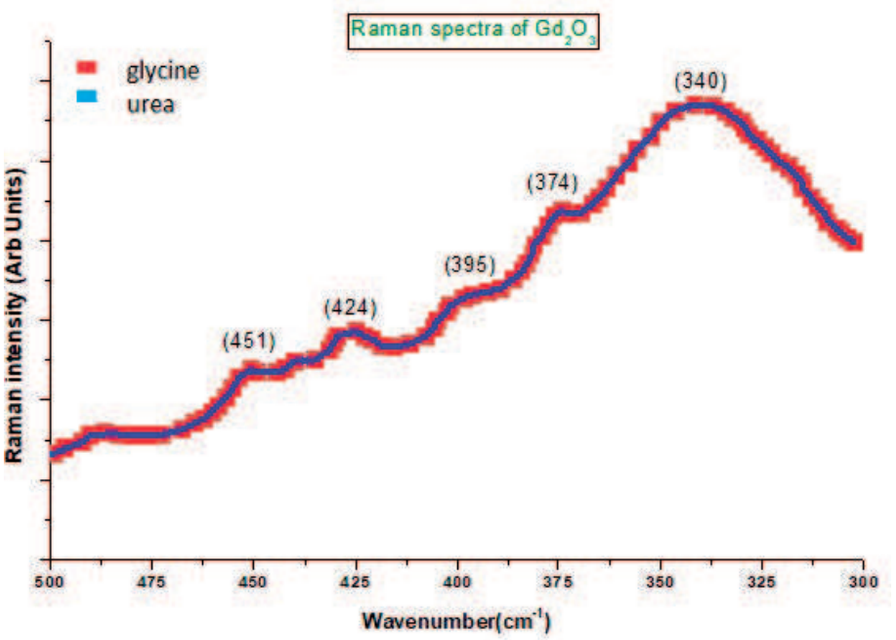

Figure 8.
Raman spectra of Gd_2O_3 nanoparticles (reproduced from [1]).

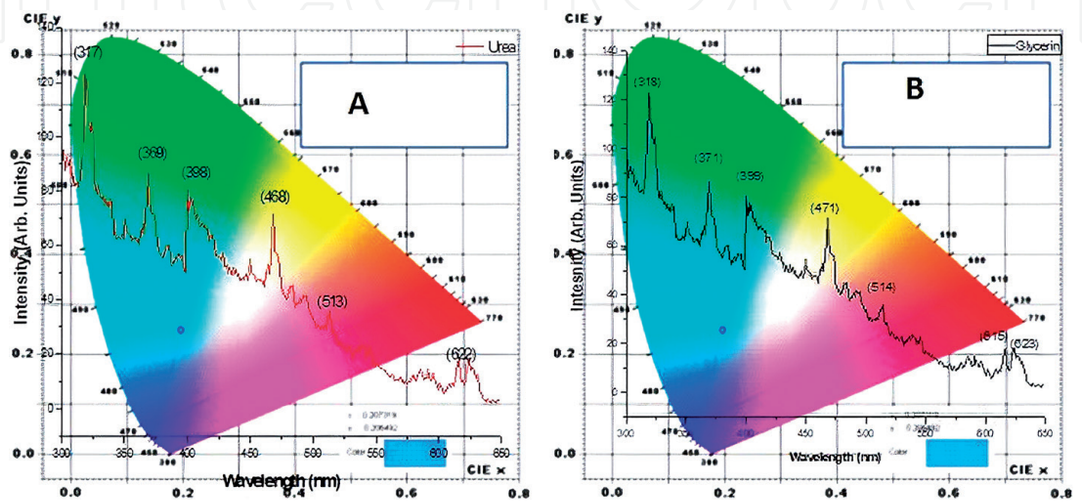

Figure 9.
Emission spectra of pure Gd_2O_3 phosphor: (A) urea and (B) glycerin (reproduced from [7]).

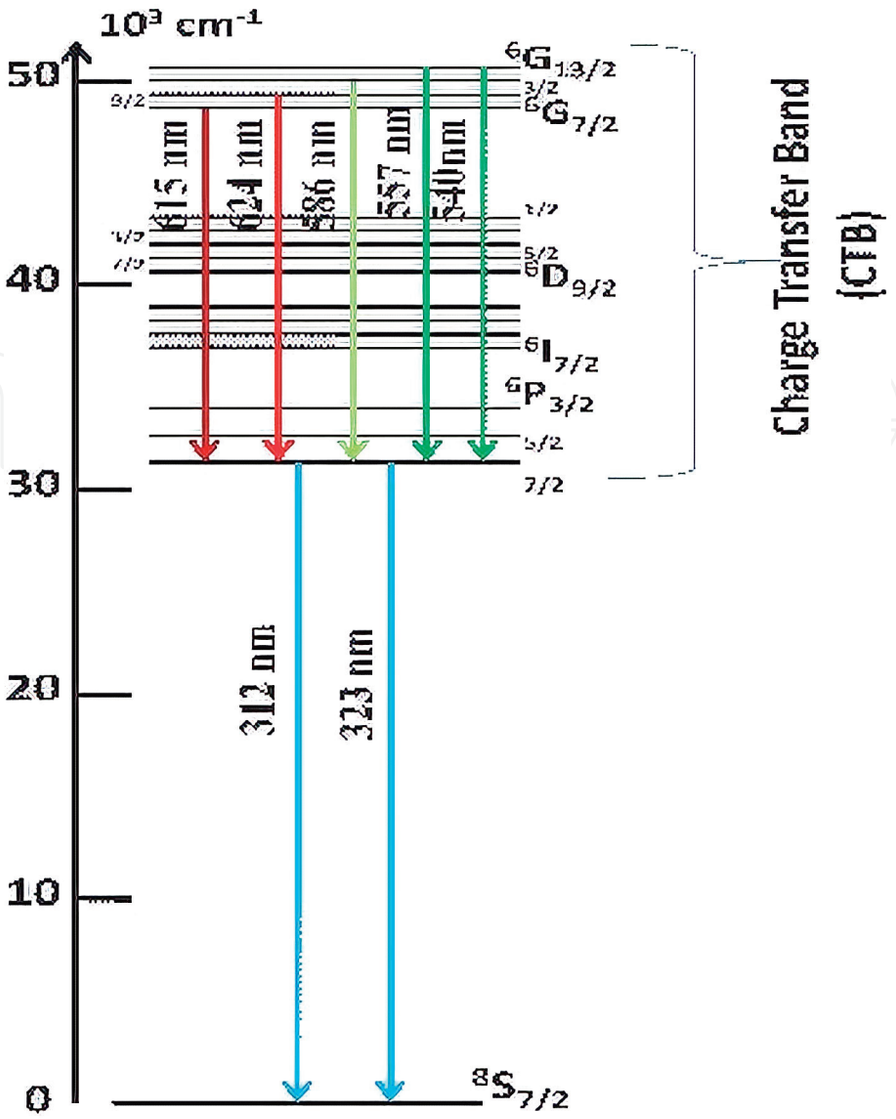

Figure 10.
Energy level diagram for emission transitions for pure Gd_2O_3 phosphor (reproduced from [7]).

3.8 Thermoluminescence study of pure Gd_2O_3 phosphor

The TL response of the Gd_2O_3 phosphor was recorded under 254 nm UV exposure and ^{60}Co gamma exposure for the phosphors prepared by both urea and glycine fuel. The TL glow curve of phosphors prepared with both the fuels was recorded under 254 nm UV exposure immediately after 5 min exposure time at 6 Cs^{-1} heating rate. For the combustion synthesized phosphor, the TL glow peak was found at 103°C and 111°C for urea and glycine fuels, respectively. For 1 kGy gamma exposure at 6 Cs^{-1} heating rate, the TL glow peak was found at 232°C and 221°C (**Figure 11**) for urea and glycine fueled phosphors, respectively [10].

Chen's peak shape method was used to determine all the kinetic parameters including order of kinetic, activation energy, shape factor, and so on [4–6, 11] (**Table 1**). The activation energy for TL glow curve for combustion synthesized both phosphors has 0.66 eV for UV exposure and 0.71 and 0.72 eV for gamma exposure. Due to gamma exposure, deeper traps were formed, which are responsible for the higher activation energy value. The phosphor follows second-order kinetics as the obtained shape factor value for UV exposure and gamma exposure was in the range of 0.49–0.52 and 0.50–0.54, respectively, which is near to 0.52 for second-order kinetics (**Table 2**).

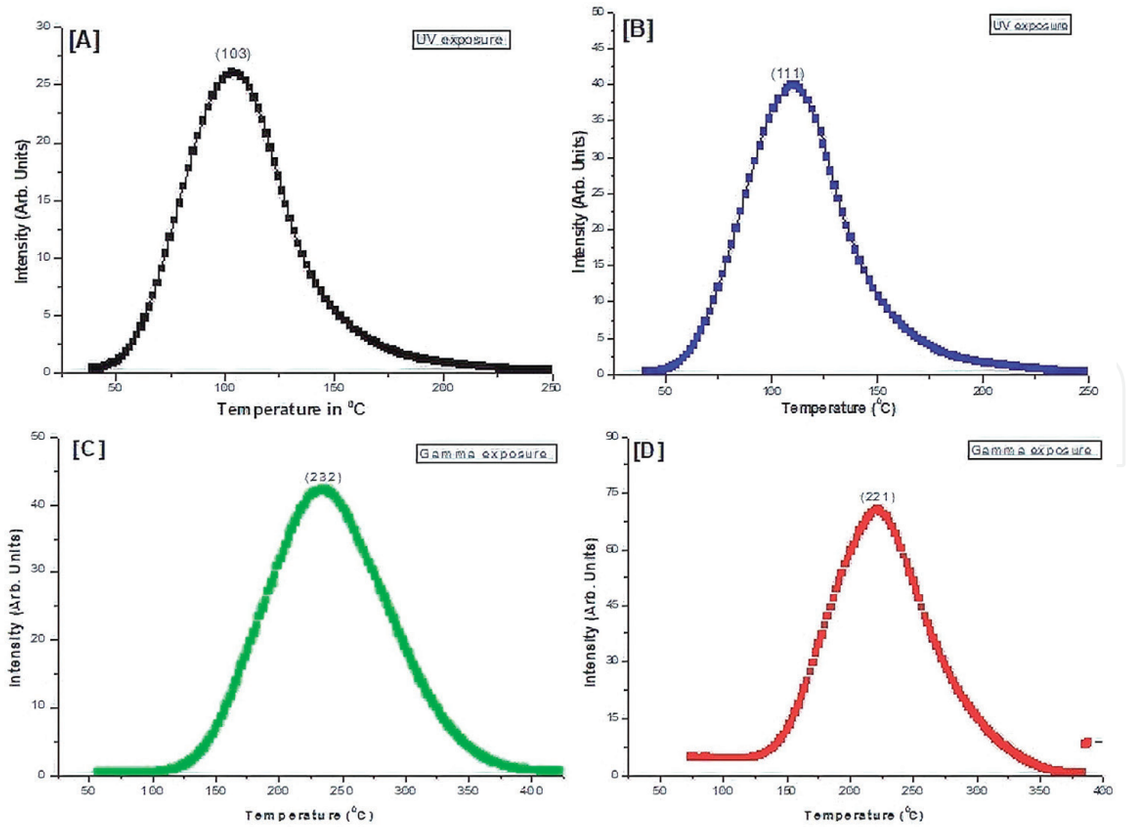

Figure 11.
TL glow curve for 6 Cs^{-1} heating rate and 10 min UV exposure with (A) urea fuel and (B) glycerin fuel. TL glow curve for 6°Cs^{-1} heating rate and 1 kGy gamma exposure (C) urea fuel and (D) glycerin fuel (Reproduced from [8]).

		Monoclinic	
		Urea	**Glycerin**
For 275 nm	X	0.207	0.207
	Y	0.206	0.206

Table 1.
X, Y coordinates for CIE diagram for Gd_2O_3 phosphor.

Exposure	**Fuel**	**μ_g**	**E (eV)**	**S (s^{-1})**
UV (254 nm)	Urea	0.49	0.66	1.4×10^{10}
	Glycerin	0.52	0.66	1.5×10^{10}
Gamma (1kGy)	Urea	0.54	0.71	9.5×10^{9}
	Glycerin	0.50	0.72	9.7×10^{9}

Table 2.
Trapping parameters for optimized TL glow curve.

4. Conclusions

The study confirms that the combustion synthesis method is suitable for large-scale production of the phosphor in minimum time. Structural characterization shows that the phosphors have monoclinic structure with particle size in the range of 8–12 nm. Phosphor synthesized by this method has homogenous particle

size distribution. X-ray Photoelectron Spectroscopy (XPS) show the Gd (3d) level consists of a spin orbit split doublet, with the Gd (3d)5/2 peak is found at 1186.74 eV. Raman spectra was recorded with excitation of 633 nm wavelength, we found a broad and intense Raman peak at 340 cm^{-1} along with less intense peaks were observed at 375, 395, 424 and 451 cm^{-1}. The emission spectra have peaks in all UV and visible regions. So that, the phosphor may behave as white light emitting phosphor, which was further confirmed by its CIE coordinates. The CIE coordinates for combustion synthesized Gd_2O_3 phosphor have values $X = 0.207$ and $Y = 0.206$, and for the glycine synthesized Gd_2O_3 phosphor $X = 0.209$ and $Y = 0.207$. The values of CIE coordinates show that the Gd_2O_3 phosphor prepared by combustion synthesis emits blue color. The TL studies of both the phosphors were carried out under UV and gamma exposure. The activation energy for 0.66 eV and 0.71–0.72 eV for UV exposure and gamma exposure respectively. The value of shape factor μg for all the TL analysis was found in between 0.45 and 0.54, which shows that the phosphors follow the second-order kinetics.

Acknowledgements

We are very grateful to NIT Raipur for XRD characterization and also thankful to Dr. Mukul Gupta for his co-operation. We are thankful to SAIF, IIT, Bombay and IIT Delhi for other characterization such as SEM, TEM, FTIR, and EDX.

Conflict of interest

The authors declare there is no conflict of interest.

Author details

Raunak Kumar Tamrakar[1*] and Kanchan Upadhyay[2]

1 Department of Applied Physics, Bhilai Institute of Technology (Seth Balkrishan Memorial), Durg, Chhattisgarh, India

2 International and Inter University Centre of Nanoscience and Nanotechnology, Mahatma Gandhi University, Kottayam, Kerala, India

*Address all correspondence to: raunak.ruby@gmail.com

References

[1] Tamrakar RK, Bisen DP, Sahu IP, Brahme N. Raman and XPS studies of combustion route synthesized monoclinic phase gadolinium oxide phosphors. Advance Physics Letter. 2014;**1**(1):1-5

[2] Tamrakar RK, Bisen DP, Sahu IP, Brahme N. Structural characterization of combustion synthesized Gd_2O_3 nanopowder by using glycerin as fuel. Advance Physics Letter. 2014;**1**(1):6-9

[3] Tamrakar RK, Bisen DP, Sahu IP, Upadhyay K, Sahu M. Structural characterization of Gd_2O_3 phosphor synthesized by solid-state reaction and combustion method using X-ray diffraction and transmission electron microscopic techniques. Journal of Display Technology. 2016;**12**(9):921-927

[4] Chen R. Thermally stimulated current curves with non-constant recombination lifetime. British Journal of Applied Physics. 1969;**2**:371-375

[5] Chen R, Kirsh Y. The Analysis of Thermally Stimulated Processes. Oxford, New-York: Pergamon Press; 1981

[6] Chen R, McKeever SWS. Theory of Thermoluminescence and Related Phenomena. London, NJ, Singapore: World Scientific Publications; 1997

[7] Tamrakar RK, Bisen DP, Upadhyay K, Sahu M, Sahu IP, Brahme N. Comparison of emitted color by pure Gd_2O_3 prepared by two different methods by CIE coordinates. Superlattices and Microstructures. 2015;**88**:382-388

[8] Tamrakar RK, Bisen DP, Upadhyay K, Sahu IP. Comparative study of thermoluminescence behaviour of Gd_2O_3 phosphor synthesized by solid state reaction and combustion method with different exposure. Radiation Measurements. 2016;**84**:41-54

[9] Tamrakar RK, Bisen DP, Brahme N. Comparison of photoluminescence properties of Gd_2O_3 phosphor synthesized by combustion and solid state reaction method. Journal of Radiation Research and Applied Science. 2014;**7**:550-559

[10] Tamrakar RK, Bisen DP, Brahme N. Characterization and luminescence properties of Gd_2O_3 phosphor. Research on Chemical Intermediates. 2014;**40**:1771-1779

[11] Chen R, Pagonis V. Thermally and Optically Stimulated Luminescence: a Simulation Approach. Chichester: Wiley; 2011